

The Fringe and Flexure Tracking Detector of the LBT LINC–NIRVANA Beam–Combiner Instrument

U. Beckmann^a, J. Behrend^a, H. Bönhardt^b, C. Connot^a, T. Driebe^a, M. Heininger^a,
T. Herbst^b, K. Hofmann^a, E. Nußbaum^a, D. Schertl^a, W. Solscheid^a, C. Straubmeier^c,
G. Weigelt^a

^aMax-Planck-Institut für Radioastronomie, Auf dem Hügel 69, 53121 Bonn, Germany;

^bMax-Planck-Institut für Astronomie, Königstuhl 17, 69117 Heidelberg, Germany;

^cI. Physikalisches Institut, Universität zu Köln, Zùlpicher Straße 77, 50937 Köln, Germany

June 17, 2004

ABSTRACT

LINC–NIRVANA is a near-infrared (1–2.4 micron) beam-combiner instrument for the Large Binocular Telescope (LBT). LINC–NIRVANA is being built by a consortium of groups at the Max-Planck-Institut für Astronomie in Heidelberg, the Osservatorio Astrofisico di Arcetri in Florence, the Universität zu Köln, and the Max-Planck-Institut für Radioastronomie in Bonn. The MPI für Radioastronomie is responsible for the near-infrared detector for the fringe and flexure tracking system (FFTS).

We describe the design and construction of the detector control electronics as well as the first laboratory measurements of performance parameters of the NIR detector for the fringe and flexure tracking system of the LBT LINC–NIRVANA instrument. This detector has to record LBT interferograms of suitable reference stars in the FOV at a frame rate of the order of 200 frames per second using, for example, 32 x 32-pixel subframes. Moreover, special noise reduction techniques have to be applied. The fringe-tracker interferograms are required for monitoring and closed-loop correction of the atmospheric optical path difference of the two LBT wavefronts (see C. Straubmeier et al., "A fringe and flexure tracking system for LINC–NIRVANA: basic design and principle of operation"¹). We will describe our laboratory measurements of maximum frame rate, readout noise, photometric stability, and other important parameters together with first measurements of laboratory simulations of LBT interferograms.

Keywords: Fringe Tracking, LBT, LINC–NIRVANA, HAWAII-1, infrared detector, noise reduction, sub-pixel sampling, non-linearity

1. INTRODUCTION

The fringe-tracker detector is located inside the LINC-NIRVANA cryostat (see P. Bizenberger et al., "The LINC-NIRVANA Cryogenic Interferometric Camera"²). The cryostat contains the cryogenic optics, which combines the light coming from the two telescopes in the interferometric focus. A set of selectable dichroic beam splitters reflects the light of a desired band to the science detector, while the other bands can be used for fringe tracking. Additional filters will be used to further select a certain wavelength range. A large FOV of approx. one arcmin can be used for fringe tracking; the physical size of the image plane is more than 210 mm. The fringe-tracker detector will be moved within the image plane on an xyz translation stage.¹

2. INSTRUMENTAL REQUIREMENTS

- Wavelength coverage:
near-infrared J, H, and K bands

- **Optical magnification and pixel size:**
The fringe-tracker detector and science detector are located in the image plane of the beam-combiner optics. The science detector is a HAWAII-2 with a pixel size of 18 micron. For the shortest wavelength of 1.14 micron the resulting F-number is $F = 31.8$ to achieve proper fringe sampling.
- **Image and detector size:**
For the F-number given above, a 1-arcmin FOV corresponds to 210.9 mm in the image plane. For fringe tracking, it is sufficient to have a small detector of 32 x 32 pixels, which can be moved on a translation stage within the large, 1-arcmin FOV. As the detector has to sample the fringes properly as discussed above, the pixel size must be the same as for the science detector. A cost-efficient solution is to use a 1-quadrant HAWAII-1 detector with 18.5 micron pixel size for fringe tracking.
- **Fringe-tracker control loop:**
The recorded interferometric PSFs contain information about the pistonic phase difference between the two telescopes. Based on simulations of the atmospheric conditions at the LBT site, frame rates of up to 200 Hz are required to correct for the optical path differences (see T. Bertram et al., "The LINC-NIRVANA fringe- and flexure tracker: PSF- and atmospheric differential piston simulations and determination algorithm"³). For correlated double sampling of the detector readout, the maximum time to read one 32 x 32 pixel frame is 2.4 ms (pixel clock frequency of 500 kHz).
- **Heat dissipation:**
The heat dissipation from the HAWAII-1 array during normal operation is negligible (≈ 1 mW). The main contribution comes from the operational amplifiers which drive the differential video signal into the coax cables of 50 Ω impedance. The total heat of less than 0.5 Watt has to be transported to the cold shields to avoid a temperature increase and thus thermal background radiation inside the dewar.

3. OVERVIEW

The detector readout electronics is directly attached to the dewar to avoid electronic interference due to long signal paths outside the dewar (see Fig. 1).

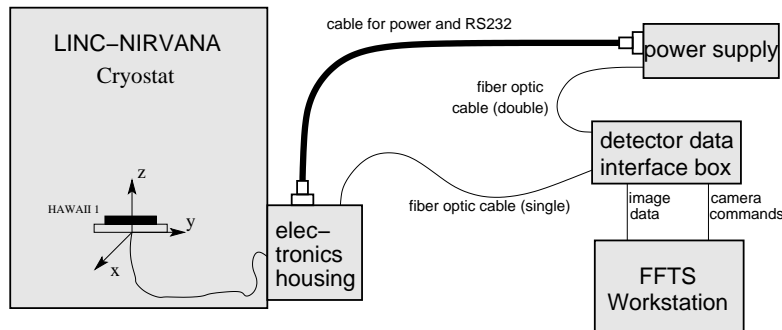


Figure 1. Fringe and flexure tracking detector

However, a cable length of 1 m is needed inside the dewar since the HAWAII array detector has to track the reference star using an xyz-stage within the 210 mm image plane, as described in Sect. 1 and shown in figure 1. The power supply is installed in a cabinet at a distance of max. 15 m cable length. There is a single cable connection between the power supply and the detector readout electronics to avoid ground loops. This cable also contains the (galvanically isolated) RS232 line for controlling the electronics. The digital image-data interferograms are transmitted to the FFTS workstation using a fiber optic cable. The FFTS interferograms are the input for the fringe-tracker control loop.

3.1. Data interface

The basic functional structure is shown in Fig. 2. Data coming from the camera are acquired by a receive process using a PCI DMA board and putting the data into a shared memory which is then accessed by the control-loop process to gain a new set of input data to be sent to the OPD control. The detector data interface box converts the optic signals to electric ones which can be used by the FFTS workstation.

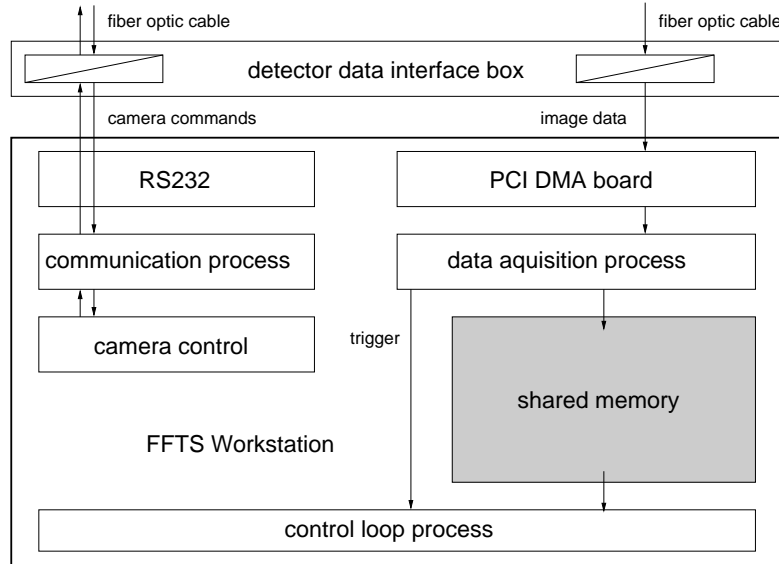


Figure 2. Interface structure

4. HAWAII-1 DETECTOR

Table 1. Detector specifications

format	1 quadrant of 512 x 512
used wavelength range	1.1 - 2.4 micron
pixel size	18.5 x 18.5 micron
subwindow size	32 x 32 pixels, location freely selectable
pixel-clock frequency	500 kHz up to 1 MHz
readout noise	15 e ⁻
frame rate	up to 200 Hz with CDS
detector quantum efficiency	> 50 %
operating temperature	77 K (LN2)

5. DETECTOR READOUT SCHEME AND READOUT MODES

- Readout scheme:

For the readout the individual detector pixels are selected by activating the horizontal and the vertical shift registers. As the horizontal shift register is faster than the vertical shift register, the detector will be oriented such that the fast direction is parallel to the fringe stripes. This has the advantage that even for

very fast readout with an increasing crosstalk between consecutive pixels (due to the limited bandwidth of the detector output) the fringe positions will not be affected.

- Readout modes:

- Correlated Double Sampling (CDS):

The detector readout sequence is: read₁ - exposure - read₂*

The final image is the difference between read₁ and read₂.

- Up the ramp:

In this mode, multiple reads are taken during the exposure time. The readout sequence is: read₁ - exposure - read₂ - exposure - . . . - read_n*

The difference between two consecutive reads gives the new image. This mode can be used for low fluxes, where even a large number of exposures (e.g., 10 or 20) does not saturate the detector.

- Read-Reset-Read:

In this mode, in the first step one line of the detector is read. It belongs to the second read of the previous image. Then, the complete line is reset within one clock cycle. The line is then read again.

This read belongs to the first read of the new image. After completing all the detector lines within the selected image area, the readout can start again with the first line.

* read₂ (read_n) is a destructive read.

6. SEQUENCER AND CLOCK GENERATION

The sequencer generates all necessary clock signals to operate the detector and the sample timing of the ADCs. It also provides a header information for each frame, which is inserted into the data stream. It supplies a galvanically decoupled RS232 interface for external control. Basically the sequencer consists of two main units: a logic cell array (LCA), which generates the fast digital signals for one detector readout, and a micro-controller, which is responsible for programming the LCA, doing the timing business between the particular readouts, and generating the header information. There are several different readout modes implemented, such as double correlated sampling(DCS) and sampling up the ramp with a multiple readout. A particular challenge concerning the FFTS was to speed up the data rate as much as possible to achieve a sufficient sample rate to the control loop. This has been realized to a frame rate of 300 double correlated frames(2x 32 x 32 pixels) per second.

7. SIGNAL TRANSMISSION BETWEEN COLD AND WARM ELECTRONICS

7.1. Wiring scheme

Clock signals are transmitted to the fanout board using twisted pair lines which are terminated at the far end. Power supply and bias voltages are driven by C-stable high bandwidth drivers. This ensures voltage stability even for high-load current changes.

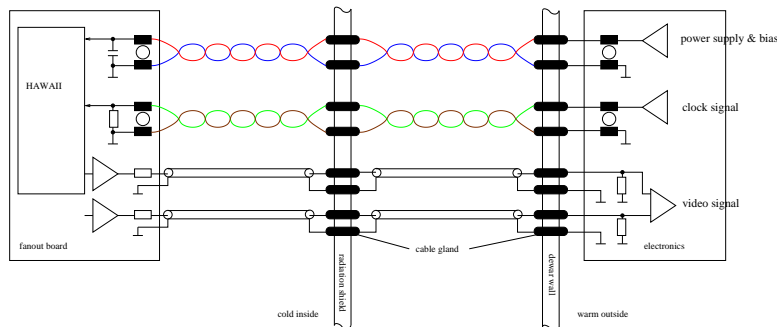


Figure 3. Wiring scheme

7.2. Active video electronics in the cold

The detector output impedance of $\approx 10\text{ k}\Omega$ is too high, and the distance of 1.5 m to the dewar outside is too long to transmit a video signal with a bandwidth of 5 MHz without preamplification. Therefore, operational amplifiers with FET inputs are used to build up a differential signal from the detector output and to drive $50\ \Omega$ transmission lines (see Sect. 2). The operational amplifiers work at the temperature of liquid nitrogen (see Fig. 4).

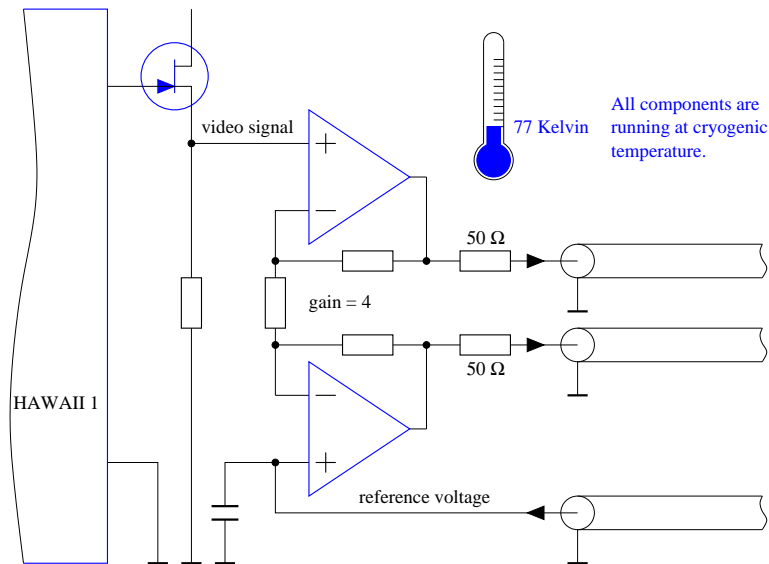


Figure 4. Preamplifier

8. NOISE REDUCTION TECHNIQUES

8.1. Analog video-signal processing

Outside the dewar the video signal has to be processed before being converted into a digital data stream (see Fig. 5).

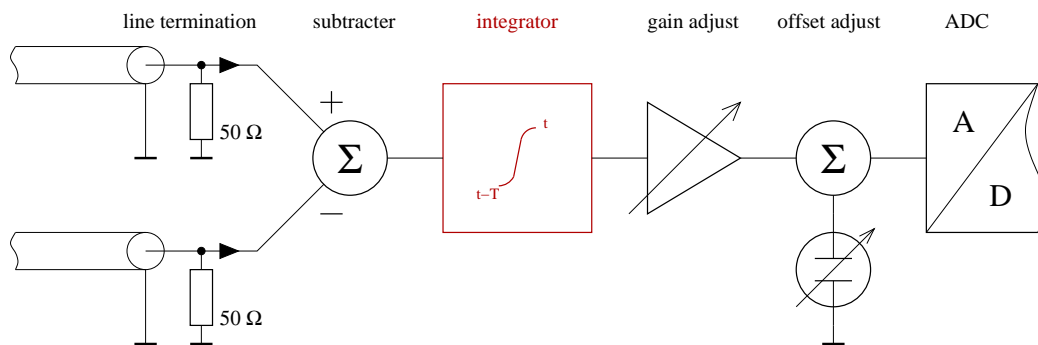


Figure 5. Signal processing

A moving average filter is used to reduce noise. The output of the filter is a continuous signal which is proportional to the average of the input during the past 100 nanoseconds. This time is equal to the sampling period of the ADC.

The filter can mathematically be described as an integrator:

$$f_{\text{out}}(t) = \frac{1}{T} \int_{t-T}^t f_{\text{in}}(t) dt \quad (1)$$

$$T = 100 \text{ ns} \quad (2)$$

The practical realization is a purely analog approximation of the integrator. Therefore, neither gate-time jitter nor digital clocks can interfere with the signal. This analog filter is part of a filtering method which is continued on the digital side.

8.2. Digital video-signal processing

The moving average filter bandwidth is matched with the ADC sampling speed. By simply adding individual ADC samples, the resulting bandwidth B is inversely proportional to the number of samples, multiplied by T :

$$B = \frac{k}{\text{number of samples} \cdot T}, \quad (3)$$

with $k \approx 1.05$, considering the imperfect analog approximation of the integrator.

After a pixel has been addressed, it takes some time for the analog signal to settle. When the signal is stable, it is sampled several times by an ADC as shown in Fig. 6. This so-called *sub-pixel sampling* has several

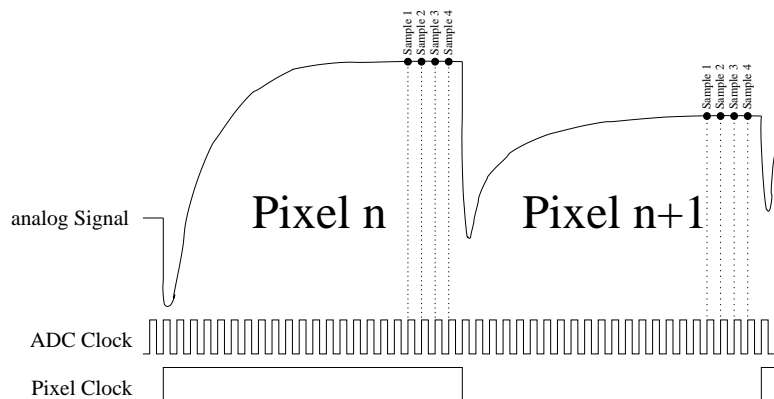


Figure 6. sub-pixel sampling

advantages:

1. Noise can be reduced by averaging the samples taken within one pixel.
2. Since the sample rate is constant the analog signal acquisition is optimally adapted to the ADC at any pixel rate.
3. The effective signal bandwidth is adapted to the pixel-clock frequency by simply changing the number of samples.

9. NON-LINEARITY

Measurements of Rockwell HAWAII-1 detectors at the MPIfR have shown that the response to illumination is not completely linear, even at lower intensities. We use a physically-based model to compensate non-linear effects in order to extend the useful dynamic range of the detector to up to 90% of the saturation level of an individual pixel. This model assumes that the detector capacitance of a pixel depends on the charge already accumulated. Due to the simplicity of the model, saturation effects are ignored. The model is represented by

$$U = \frac{Q}{C_0 + \alpha Q}, \quad (4)$$

where U is the measured pixel voltage, Q is the accumulated pixel charge, C_0 the capacitance of an empty pixel after reset, and α , a non-linearity factor. For practical reasons the following equation is used to model flatfield and non-linear properties of a pixel:

$$I_R = \frac{aI_C}{1 + bI_C}, \quad (5)$$

where I_R is the measured raw intensity, I_C the calibrated intensity, a the relative gain, and b the non-linearity factor.

A non-linearity map contains three values for each pixel. One value defines the limit up to which the non-linear behavior can be compensated for (e.g., modeled by Eq. 5). The other two values define parameters a and b from Eq. 5. Before non-linearity compensation, global bias, pixel bias, and $1/f$ noise must be corrected. From an image series taken with a HAWAII-1 detector the pixel at position (63/100) is used to demonstrate the gain in dynamic range by compensating the non-linearity. In Fig. 7 it can be seen that for the flatfield compensation the non-linearity exceeds the $\pm 0.5\%$ limit at about 19000 DU. If the non-linearity is compensated for by using the inverse of Eq. 5 the useful dynamic range extends to 26000 DU.

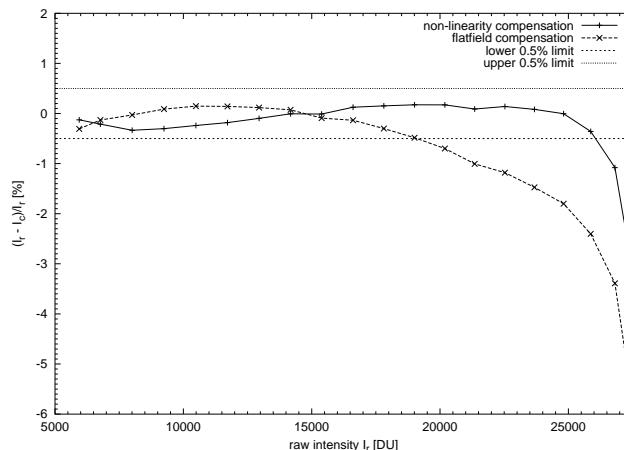


Figure 7. Pixel non-linearity

10. LABORATORY TESTS

We carried out laboratory tests to simulate the instrument operation with the constraints mentioned in the "Instrumental Requirements" (see Sect. 2). The measurements were performed under the following conditions:

- Readout mode: CDS (see Sect. 2)
- Pixel clock: 500 kHz and 1 MHz
- Image size: 32 x 32 pixels, starting at row 3 and column 3 of the detector
- Video-cable length: 2 m differential between fanout board and detector-readout electronics
- Exposure time: set to minimum, which is equivalent to the time between two detector readouts

The detector clocking was optimized for speed. For example, additional delays after the reset pulse which improve the RON were not applied. Therefore, the readout noise increased by $\approx 10\%$ over our standard clocking scheme. The results achieved are shown in Tab. 2:

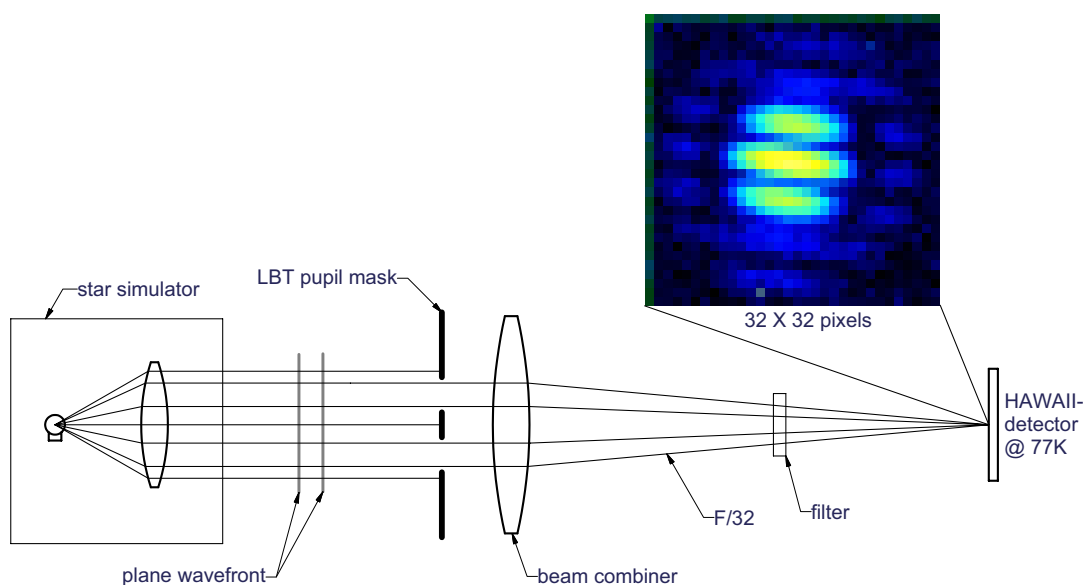
Table 2. Detector measurements

RON (double correlated)	15.5 e ⁻ @ 450 kHz, 30 e ⁻ @ 1 MHz
RON detector electronics	2 e ⁻
conversion factor	2.11 $\frac{e^-}{DN}$
full well capacity	≈ 110,000 e ⁻ @ $U_{\text{reset}} = 0.5$ V
1 % nonlinearity	≈ 39,000 e ⁻ , uncorrected
1 % nonlinearity	≈ 90,000 e ⁻ , corrected
number of bad pixels	1304 (whole quadrant)
clusters of bad pixels (≥ 4)	≈ 25 (whole quadrant)
CDS frame rate (32 x32 pixel field)	320 Hz

10.1. Laboratory simulations of the LBT LINC-NIRVANA interferograms

With a laboratory test setup (see Fig. 8) we recorded the simulated LN interferograms. A "star simulator" produces the plane wavefront of a single star. The following pupil mask simulates the relative LBT pupil function. An F/32 beam is focussed on the fringe-tracker detector by the beam-combiner lens. A typical interferogram of a faint single star can be seen in figure 8. This raw image shows a fringe pattern within the core of the Airy disk and the first Airy ring.

A typical interferogram of a faint single star can be seen in figure 8. This raw image shows a fringe pattern within the core of the Airy disk and the first Airy ring.

**Figure 8.** Fringe-tracker laboratory test setup

REFERENCES

1. C. Straubmeier, T. Bertram, A. Eckart, Y. Wang, L. Zealouk, T. M. Herbst, D. R. Anderson, R. Ragazoni, and G. Weigelt, *A fringe and flexure tracking system for LINC-NIRVANA: basic design and principle of operation*, Universität zu Köln (Germany), Max-Planck-Institut für Astronomie (Heidelberg, Germany), Max-Planck-Institut für Radioastronomie Bonn (Germany), Osservatorio Astrofisico di Arcetri (Italy).
2. P. Bitzenberger, D. R. Anderson, H. Baumeister, U. Beckmann, E. Diolaiti, T. M. Herbst, W. Laun, L. Mohr, V. Naranjo, and C. Straubmeier, *The LINC-NIRVANA Cryogenic Interferometric Camera*, Universität zu Köln (Germany), Max-Planck-Institut für Astronomie (Heidelberg, Germany), Max-Planck-Institut für Radioastronomie (Bonn, Germany), Osservatorio Astrofisico di Arcetri (Italy).
3. T. Bertram, C. Straubmeier, D. R. Anderson, C. Arcidiacono, U. Beckmann, A. Eckart, and T. M. Herbst, *The LINC-NIRVANA fringe- and flexure tracker: PSF- and atmospherical differential piston simulations and determination algorithm*, Universität zu Köln (Germany), Max-Planck-Institut für Astronomie (Heidelberg, Germany), Max-Planck-Institut für Radioastronomie (Bonn, Germany), Univ. degli Studi di Firenze (Italy).